Ray-Optical Calculation of Edge Diffraction in Unstable Resonators

CARLOS E. SANTANA, MEMBER, IEEE, AND LEOPOLD B. FELSEN, FELLOW, IEEE

Abstract—**A previously developed ray-optical theory for calculation of modal reflection and coupling coefficients due to edge discontinuities in homogeneously or inhomogeneously filled parallel-plane waveguides is generalized to waveguides with nonplanar boundaries. Treated in particular are the reflections from the open ends of a bilaterally truncated waveguide whose convex walls are confocal hyperbolas. This open configuration serves as a model for unstable optical resonators with cylindrical mirrors. The ray optically determined modal reflection and coupling coefficients for mirrors with large Fresnel number are shown to reduce to those in a previously employed local parallel-plane approximation when the Fresnel numbers are moderate. The analysis quantifies proposed ray-optical models for explaining the influence of edge diffraction on the behavior of the resonant modes.**

I. Introduction

BY A FAIRLY recent generalization [1], [2], it has been shown how high-frequency ray-optical techniques can be adapted to the analysis of scattering by localized discontinuities (small obstacles, edges, etc.) in waveguides or ducts filled with homogeneous or inhomogeneous dielectric media. Basic to the technique is the ray-optical formulation of the waveguide Green's function, i.e., the radiation from a source with an isotropic radiation pattern. This is then generalized to nonisotropic sources with a radiation pattern $f(\theta)$,[1] where θ is the angle measured from the waveguide axis y. A localized discontinuity may be characterized by its free-space diffraction pattern $\bar{f}(\theta,\theta_i)$ when the incident field is a uniform plane wave impinging from the direction θ_i. When the discontinuity is placed inside the waveguide and illuminated by an incident waveguide mode, which can locally be decomposed into uniform plane waves with characteristic angles $\theta_j^{\pm}$, the resulting $\bar{f}(\theta,\theta_j^{\pm})$ constitutes an equivalent nonisotropic source whose excitation of modal fields may be calculated from the solution referred to above. In this manner, one derives by ray-optical techniques the modal reflection, transmission, and coupling coefficients (the scattering matrix elements) for a discontinuity inside the waveguide. The lowest-order, single diffraction solution so obtained may be refined by accounting for multiple diffraction effects due to interaction between the singly diffracted fields and the waveguide boundaries. For details of the method, the reader is referred to previous work [2]–[6].

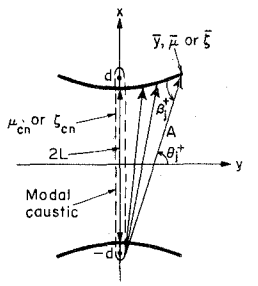

Fig. 1. Unstable resonator with hyperbolic mirrors. The resonator axis lies along x and the waveguide axis along y. A typical modal caustic, an ellipse with foci at $x = \pm d$, is shown, together with one congruence of upgoing modal rays. Ray A strikes the upper edge, and θ_j^+ is the propagation angle of the corresponding local plane wave field in the jth mode. A similar congruence of downgoing modal rays has been omitted, as has the corresponding picture for the left half of the resonator. For very slender caustics, all modal rays appear to originate at the foci. The edges of the mirrors are located at $\pm\bar{y}$, $\bar{\mu}$, or $\bar{\zeta}$ in the various coordinate systems defined in the text; the analogous designation for the modal caustic is μ_{cj} or ζ_{cj}.

The ray optical technique has already been applied to the study of discontinuities in waveguides of various types [6], [7]. In the present paper, it is shown how it can be applied to the important problem of unstable open optical resonators. Because of their good mode selectivity and large mode volume, such structures appear to be most promising for use with laser sources of high and even moderate gain [8]. By recent studies performed independently in the United States [9], [10] and the Soviet Union [11], it has been shown that the unstable resonator can be regarded as a waveguide whose boundaries are the convex resonator mirrors, and whose axis is transverse to the resonator axis (Fig. 1). Resonance in this open waveguide is established by self-consistent reflection of a propagating waveguide mode between the edge discontinuities formed by the rims of the mirrors. Although the waveguide is very strongly overmoded, it has been shown that near the cutoff condition,

Manuscript received October 15, 1976; revised October 11, 1977. This work was supported in part by the National Science Foundation under Grant ENG-7522625, by the Joint Services Electronics Program under Contract F 44620-69-C-0047, and in part by the Advance Research Projects Agency of the Department of Defense, monitored by the Office of Naval Research, under Contract N00014-67-A-0438-0017. It represents part of a dissertation submitted by C. Santana to the Polytechnic Institute of New York, Brooklyn, NY, in partial fulfillment of the requirements for the Ph.D. degree in electrophysics.

C. Santana was with the Department of Electrical Engineering and Electrophysics, Polytechnic Institute of New York, Farmingdale, NY. He is now with the Institute of Space Research, National Council of Research, 12.200-Sao Jose Campos, San Paulo, Brazil.

L. B. Felsen is with the Department of Electrical Engineering, Polytechnic Institute of New York, Farmingdale, NY 11735.

[1] Although three-dimensional problems can be treated by this method, we consider here only the two-dimensional z-independent case.

0018-9480/78/0200-0101$00.75

which is of interest for the resonator problem, mode coupling due to the mirror edges is confined essentially to adjacent modes. Thus a very simple model involving selective coupling between two waveguide modes has been developed, and has been found capable of explaining the intricate eigenmode loss behavior determined by numerical solution of the resonator integral equation [9], [10]. While the role of mode coupling has been alluded to in the Russian work [11], it has not been incorporated into their analysis. The Soviet calculations are based on a single mode analysis, which is adequate only near eigenmode loss minima, and does not provide the peculiar interconnections between successive loss minima found in the numerical results.

A further attribute of our analysis [9], [10] is the avoidance of the resonator integral equation, which forms the basis of the Soviet approach to the waveguide problem as originally formulated by Weinstein [12], and followed thereafter by others in the Soviet Union [11], [13]. By avoiding the integral equation, it is possible to decompose the unstable resonator problem into conventional microwave network constituents involving propagation (waveguide) and discontinuity regions. By this separation, one may also extend the analysis to resonator configurations which are filled with inhomogeneous and/or active materials, and to mirror shapes which depart from the conventional circular contours. These aspects are presently under investigation.

While the ray optical principle of localization is consonant with the microwave network approach, the reflection and coupling coefficients due to the mirror edges were previously [9], [10] not calculated by the ray-optical method described earlier. Instead, these coefficients were taken from Weinstein [12] by modeling the region near the edges locally as an open-ended parallel-plane waveguide. Since the ray-optical method synthesizes the reflection and coupling coefficients by direct edge scattering, it is of interest to examine whether the two procedures yield the same result. This is especially important for resonators with moderately large Fresnel numbers,[2] where the local parallel-plane approximation near the edges is more difficult to justify since the slanting of the convex waveguide boundaries is then not negligible. It will be shown that the single-diffraction ray optically evaluated reflection and coupling coefficients are identical with those obtained by Weinstein from the rigorous solution of the open-ended parallel-plane waveguide problem when the characteristic angle of the incident mode is not almost 90° with respect to the waveguide walls; this is the range of interest for the moderately large Fresnel number regime. This confirmation then suggests that the single diffraction ray-optical model may be used with confidence for large and very large Fresnel numbers where the local parallel-plane approximation is clearly in doubt. The reflection and coupling coefficients derived here may then be regarded as more reliable than any of those available heretofore. Although the ray optical edge diffraction mechanism has been proposed as an explanation of the numerically observed eigenmode loss behavior [14]–[16], this fact has not been incorporated into a systematic modal theory. Such an incorporation is performed in this paper.

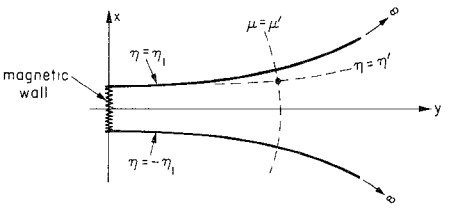

Fig. 2 Bisected waveguide configuration

The presentation follows the format outlined at the beginning of this Introduction. The Green's function for the waveguide with hyperbolic boundaries is developed in Section II. This is followed in Section III by modifications required to accommodate a nonisotropic source with radiation pattern $f(\theta)$. Section IV deals with the local plane-wave decomposition of the incident mode field impinging onto the edges of the truncated waveguide boundaries, and the subsequent calculation of the edge diffraction pattern function $f(\theta,\theta_j^{\pm})$. This information is then utilized for extraction of the modal reflection and coupling coefficients. The analysis is similar to that performed previously for a parallel-plane waveguide filled with a plane-stratified medium [2]. However, in the present instance it is necessary to perform a generalization to account for nonplanar boundaries. Concluding remarks are made in Section V.

II. The Waveguide Green's Function

We seek a solution of the equation

$$(\nabla^2 + k^2)G(\rho,\rho') = -\delta(\rho - \rho'), \qquad \rho = (\mu,\eta) \tag{1}$$

subject to the boundary conditions

$$\frac{\partial G}{\partial \mu} = 0 \quad \text{at} \quad \mu = 0 \tag{1a}$$

$$G = 0 \quad \text{at} \quad \eta = \pm\eta_1 \tag{1b}$$

and a radiation condition at $\mu \to \infty$. A time dependence $\exp(-i\omega t)$ is suppressed. Here, μ and η are constant coordinate surfaces in an elliptic coordinate system (Fig. 2). The boundary condition (1b) identifies G as the single-component electric field $E \equiv E_z$, and the source as a suitably normalized line of z-directed electric currents. Since we shall be interested only in field solutions which are even with respect to the $y = 0$ plane, the boundary condition in (1a) has been imposed and effectively bisects the waveguide.

In terms of waves propagating along the y (or μ) directions, the Green's function can be represented as:

$$G(\rho,\rho') = \sum_n \frac{\Phi_n(\eta)\Phi_n(\eta')}{N_n^2} g_n(\mu,\mu') \tag{2}$$

where

$$N_n^2 = \int_{-\eta_1}^{\eta_1} \Phi_n^2(\eta)\, d\eta \tag{2a}$$

[2] The Fresnel number is defined as $N = k\bar{y}^2/4\pi L$; k is the wavenumber and $\bar{y}$ and L are given in Fig. 1.

is the squared normalization constant for the eigenfunctions $\Phi_n(\eta)$. The latter satisfy the source-free one-dimensional equation

$$\left[\frac{d^2}{d\eta^2} + h^2(b_n^2 - \sin^2\eta)\right]\Phi_n(\eta) = 0, \qquad h = kd \tag{3}$$

with b_n representing the modal eigenvalue and

$$\Phi_n(\pm\eta_1) = 0. \tag{3a}$$

The one-dimensional Green's function $g_n(\mu,\mu')$ satisfies the source-excited equation

$$\left[\frac{d^2}{d\mu^2} + h^2(\cos h^2\mu - b_n^2)\right]g_n(\mu,\mu') = -\delta(\mu - \mu') \tag{4}$$

with

$$\frac{dg_n}{d\mu} = 0 \quad \text{at} \quad \mu = 0,$$

$$\text{radiation condition at } \mu \to \infty. \tag{4a}$$

The eigenfunctions $\Phi_n(\eta)$ were determined previously [9]. Assuming that the turning points $\eta_{cn} = \pm\sin^{-1} b_n$ lie outside the domain $-\eta_1 < \eta < \eta_1$ (this is the case for the modes of interest), and since h is large, one may employ the WKB approximations for $\Phi_n(\eta)$:

$$\Phi_n(\eta) \sim \frac{\sin\left[h\int_\eta^{\eta_1}\psi_n(\tau)\,d\tau\right]}{[\psi_n(\eta)]^{1/2}},$$

$$\psi_n(\eta) = (b_n^2 - \sin^2\eta)^{1/2} \tag{5}$$

with b_n defined by (3a) via

$$h\int_{-\eta_1}^{\eta_1}\psi_n(\tau)\,d\tau = n\pi, \qquad n = \text{integer} \tag{5a}$$

or approximately as [9],

$$b_n^2 \approx 2\frac{n\pi - 2kL}{k\ln M} + 1, \tag{5b}$$

where

$$M = 1 + 2\gamma + 2\sqrt{\alpha}, \qquad \alpha = \gamma + \gamma^2, \qquad \gamma = L/r. \tag{5c}$$

M is the linear magnification, and γ is the ratio of the resonator half-length L, measured along the x axis, to the radius of curvature r of the mirrors on this axis. When the sine function in (5) is expressed as the sum of two exponentials, and the result is then substituted into (2a), one observes that two of the resulting integrals contribute negligibly because of rapidly fluctuating integrands. Thus

$$N_n^2 \sim \frac{1}{2}\int_{-\eta_1}^{\eta_1}\frac{d\tau}{\psi_n(\tau)} \approx \frac{\ln M}{2} - (b_n^2 - 1)\left(\frac{\ln M}{8} + \frac{\alpha^{1/2}}{4}\right). \tag{6}$$

The evaluation of the integral in (6) is based on the approximation $b_n \approx 1$, which applies to the modes of interest (see [9]).

The modal Green's function $g_n(\mu,\mu')$ can be constructed in terms of solutions $\overleftarrow{F}_n$ and $\vec{F}_n$, which satisfy the source-free equation (4), and the boundary conditions at $\mu = 0$ and $\mu \to \infty$, respectively [17]:

$$g_n(\mu,\mu') = \frac{\overleftarrow{F}_n(\mu_<)\vec{F}_n(\mu_>)}{-W(\overleftarrow{F}_n,\vec{F}_n)}, \qquad W = \overleftarrow{F}_n\frac{d\vec{F}_n}{d\mu} - \vec{F}_n\frac{d\overleftarrow{F}_n}{d\mu} \tag{7}$$

where $\mu_<$ and $\mu_>$ denote the lesser and greater of the values of μ and μ', respectively. Since $0 \le \mu \ll 1$ in the range of interest (the waveguide region is to be truncated at $\bar{\mu} \ll 1$ to form the resonator with finite mirrors), one may approximate $\cosh^2\mu \approx 1 + \mu^2$. Introducing

$$\zeta = (2h)^{1/2}\mu,$$

$$\hat{g} = (2h)^{1/2}g,$$

$$p_n = \frac{h}{2}\mu_{cn}^2 = \frac{h}{2}(b_n^2 - 1) \tag{8}$$

where μ_{cn} locates the turning point (modal caustic) of the approximated differential equation (4), one may write

$$\left(\frac{d^2}{d\zeta^2} + \frac{\zeta^2}{4} - p_n\right)\hat{g}_n(\zeta,\zeta') = \delta(\zeta - \zeta') \tag{9}$$

with boundary conditions corresponding to (4a). The solutions $\overleftarrow{F}_n$ and $\vec{F}_n$ are now constructed in terms of parabolic cylinder functions [10], and yield

$$\hat{g}_n = e^{\pi p_n/2}(2^{ip_n})\frac{\Gamma\left(\frac{1}{4} + i\frac{p_n}{2}\right)}{\Gamma\left(\frac{1}{4} - i\frac{p_n}{2}\right)}$$

$$\cdot\left\{D_\nu(z_<) + i(2^{-ip_n})\frac{\Gamma\left(\frac{1}{4} - i\frac{p_n}{2}\right)}{\Gamma\left(\frac{1}{4} + i\frac{p_n}{2}\right)}\cdot D_{-\nu-1}(iz_<)\right\}D_\nu(z_>) \tag{10}$$

where

$$z = \zeta e^{-i\pi/4} \qquad \nu = -\tfrac{1}{2} - ip_n. \tag{10a}$$

For observation points $\zeta \gg |\zeta_{cn}|$, $\zeta_{cn} = 2|p_n|^{1/2}$, i.e., far enough from the modal caustic at ζ_{cn}, one may employ the WKB approximations for the parabolic cylinder functions

$$\Lambda^{(1)}D_\nu(z) \sim [\phi_n(\zeta)]^{-1/2}$$

$$\cdot\exp\left[i\int_{\zeta_{cn}}^{\zeta}\phi_n(\xi)\,d\xi + i\pi/4\right] \tag{11a}$$

$$\Lambda^{(2)}D_{-\nu-1}(iz) \sim [\phi_n(\zeta)]^{-1/2}$$

$$\cdot\exp\left[-i\int_{\zeta_{cn}}^{\zeta}\phi_n(\xi)\,d\xi - i\pi/4\right] \tag{11b}$$

where

$$\phi_n(\zeta) = \left(\frac{\zeta^2}{4} - p_n\right)^{1/2} \tag{11c}$$

$$\Lambda^{(1),(2)} \equiv \sqrt{2}\exp\left[\frac{\pi p_n}{4} \pm i\frac{\pi}{8}\right]$$

$$\cdot\exp\left[\pm i\frac{p_n}{2}(\ln p_n - 1)\right] \tag{11d}$$

and the phase reference in (11a) and (11b) has been taken at ζ_{cn}. Defining

$$B_n = \frac{\exp(-i\pi/4)}{2^{-ip_n}} \frac{\Gamma\left(\frac{1}{4} + i\frac{p_n}{2}\right)}{\Gamma\left(\frac{1}{4} - i\frac{p_n}{2}\right)} \exp[ip_n(1 - \ln p_n)] \quad (12)$$

one may write for (10)

$$\hat{g}_n \sim \frac{\exp\left[i\int_{\xi<}^{\xi>} \phi_n(\xi)\,d\xi\right]}{-2i[\phi_n(\zeta)\phi_n(\zeta')]^{1/2}} + B_n \frac{\exp\left[i\int_{\xi<}^{\xi>} \phi_n(\xi)\,d\xi + 2i\int_{\zeta_{cn}}^{\xi<} \phi_n(\xi)\,d\xi\right]}{-2i[\phi_n(\zeta)\phi_n(\zeta')]^{1/2}}. \quad (13)$$

The first term in (13) represents the direct contribution from the source point at ζ' to the observation point at ζ, while the second term describes a wave that has traveled from the source point to the modal caustic and thence to the observation point. The reflection coefficient due to the caustic, as seen from the observation point, is given by the ratio of the reflected and incident waves as:

$$\tilde{R}_n(\zeta) \sim B_n \exp\left[2i\int_{\zeta_{cn}}^{\zeta} \phi_n(\xi)\,d\xi\right], \quad (14)$$

which has been given previously [10].

When the results in (5) and (13) are substituted into (2), one obtains the WKB approximated Green's function for $\zeta < \zeta'$:

$$G \sim \sum_n \frac{\sin\left[h\int_{\eta}^{\eta_1} \psi_n(\tau)\,d\tau\right] \sin\left[h\int_{\eta'}^{\eta_1} \psi_n(\tau)\,d\tau\right]}{N_n^2[\psi_n(\eta)\psi_n(\eta')]^{1/2}} \cdot \frac{\exp\left(-i\int_{\xi'}^{\xi} \phi_n(\xi)\,d\xi\right) + B_n \exp\left[-i\int_{\xi'}^{\xi} \phi_n(\xi)\,d\xi + 2i\int_{\xi_{cn}}^{\xi} \phi_n(\xi)\,d\xi\right]}{-2i(2h)^{1/2}[\phi_n(\zeta)\phi_n(\zeta')]^{1/2}}. \quad (15)$$

III. Response to a Directive Source

The Green's function in (15) represents the field excited by a line source of strength

$$G_0(|\rho - \rho'|) = \frac{i}{4} H_0^{(1)}(k|\rho - \rho'|) \sim \frac{i}{4}\left(\frac{2}{\pi k|\rho - \rho'|}\right)^{1/2} \cdot \exp[ik|\rho - \rho'| - i\pi/4]. \quad (16)$$

When the source has a radiation pattern $f(\theta)$ so that its far field is

$$\bar{G}_0 \sim G_0 f(\theta), \quad (17)$$

it can be shown by a generalization of the procedure in [2] that the response in the waveguide may be calculated by decomposing the sourcepoint dependent eigenfunction $\Phi_n(\eta')$ into its local plane-wave constituents, and multiplying these by $f(\pi + \theta_n'^{\pm})$, where $\theta_n'^{\pm}$ are the propagation angles of the local plane waves in the nth mode at the source point. Thus the field $\bar{G}$ at $\zeta < \zeta'$, produced when the directive source in (17) is placed inside the waveguide, is given by

$$\bar{G} = \sum_n \frac{[f(\pi + \theta_n'^{-})u_{n2}(\eta') + f(\pi + \theta_n'^{+})u_{n1}(\eta')]}{N_n^2} \Phi_n(\eta) g_n(\mu,\mu') \quad (18)$$

where $\Phi_n = u_{n1} + u_{n2}$, and

$$u_{n1,2}(\eta) \sim \mp \frac{\exp[\mp ih\int_{\eta}^{\eta_1} \psi_n(\tau)\,d\tau]}{2i[\psi_n(\eta)]^{1/2}}. \quad (18a)$$

If the source is located on the lower wall or the upper wall, one puts $f(\pi + \theta_n'^{+}) = 0$ and $f(\pi + \theta_n'^{-}) = 0$, respectively [2]; the pattern functions now represent the respective far zone fields of the source in the presence of the boundary whereon it is situated.

IV. Reflection Coefficient for the Open-Ended Waveguide

A. General Formulation for Large Fresnel Numbers

When the waveguide in Fig. 2 is truncated at $\zeta = \bar{\zeta}$, reflection occurs from the open end. By the ray-optical method, the modal reflection and coupling coefficients are calculated from the single-edge diffraction patterns. This requires first a determination of the local plane-wave fields that illuminate the edges. Assume that an incident field E_j in the jth mode is normalized so that

$$E_j(\eta,\zeta) \sim E_j^+(\eta,\zeta) + E_j^-(\eta,\zeta) \quad (19)$$

where E_j^+ and E_j^- represent the local plane wave constituents (modal-ray congruences) traveling toward the upper and lower boundaries, respectively.

$$E_j^{\pm}(\eta,\zeta) = \mp\{2iN_j[\psi_j(\eta)\phi_j(\zeta)]^{1/2}\}^{-1} \cdot \exp\left\{\mp ih\int_{\eta}^{\eta_1} \psi_j(\tau)\,d\tau + i\int_{\zeta_{cj}}^{\zeta} \phi_j(\xi)\,d\xi\right\}. \quad (19a)$$

Then the strengths of the local plane-wave fields striking the upper and lower edges are $E_j^+(\eta_1,\bar{\zeta})$ and $E_j^-(-\eta_1,\bar{\zeta})$, respectively; note that when $\eta = -\eta_1$, the first exponential in (21a) reduces to $(-1)^j$, in view of (5a). The angles of incidence $\beta_j^{\pm}$ of the local modal plane-wave fields with respect to the tangent planes to the mirrors at the edges are obtained from the orientation of the phase gradients (i.e., the modal rays) in (19a); as shown in Fig. 1, the modal rays are tangent to the modal caustic. It is shown in Appendix I that

$$\cos\beta_j^+ \approx \frac{2\bar{\mu}^2 + 1 - b_j^2}{2\bar{\mu}\cos\eta_1}, \qquad b_j^2 = 1 + \mu_{cj}^2, \quad \mu_{cj}^2 \ll 1. \quad (20)$$

The diffraction field due to the upper edge, observed at an angle β with respect to the tangent plane at the edge, is now given by (17) with the pattern function

$$\bar{f}^+(\beta^+,\beta_j^+) = E_j^+(\eta_1,\bar{\zeta}) V(\beta^+,\beta_j^+) \quad (21)$$

where $V(\beta^+,\beta_j^+)$ is the known diffraction coefficient for a perfectly reflecting half-plane illuminated by a unit strength plane wave field incident at the angle β_j^+ [19]:

$$V(\beta,\beta_j) = -\sec\frac{\beta - \beta_j}{2} + \sec\frac{\beta + \beta_j}{2}, \qquad \beta \pm \beta_j \not\approx \pi. \quad (22)$$

The excitation of the nth waveguide mode by the equivalent directive line source with $\bar{f}^+(\beta^+,\beta_j^+)$ located at the upper edge involves the pattern function $f(\pi+\theta_n'^+)$ in (18), with $f(\pi+\theta_n'^-)$ set equal to zero. When referred to the edge-centered coordinate system, $f(\pi+\theta_n'^+)$ is equivalent to $\bar{f}^+(\beta_n^+,\beta_j^+)$, where β_n^+ is the modal ray angle for the nth mode at the edge. Similar considerations lead to the pattern function $f(\pi+\theta_n'^-)\rightarrow\bar{f}^-(\beta_n^-,\beta_j^-)$ descriptive of the lower edge. The resulting nth mode amplitude excited by both edges represents the coupling coefficient Γ_{jn} due to an incident jth mode field, while Γ_{jj} represents the reflection coefficient in the incident mode.

When the preceding results are substituted into (18), one obtains for the total reflected field E_{rj} due to an incident mode j:

$$E_{rj}\sim\sum_n\Gamma_{jn}\{N_n[\psi_n(\eta)\phi_n(\zeta)]^{1/2}\}^{-1}\cdot\sin\left[h\int_{\eta}^{\eta_1}\psi_n(\tau)\,d\tau\right]\exp\left[-i\int_{\zeta_{cn}}^{\bar{\zeta}}\phi_n(\xi)\,d\xi\right]\tag{23}$$

where

$$\Gamma_{jn}=\frac{[1+(-1)^{n+j}]V(\beta_n,\beta_j)}{8i(2h)^{1/2}[\psi_n(\eta_1)\psi_j(\eta_1)\phi_n(\bar{\zeta})\phi_j(\bar{\zeta})]^{1/2}N_nN_j}\cdot\exp\left[i\int_{\zeta_{cn}}^{\bar{\zeta}}\phi_n(\xi)\,d\xi+i\int_{\zeta_{cj}}^{\bar{\zeta}}\phi_j(\xi)\,d\xi\right]\tag{24}$$

and it has been recognized that $\beta_n^+=\beta_n^-\equiv\beta_n$, $\beta_j^+=\beta_j^-\equiv\beta_j$. The reflected modal fields have here been normalized in the same manner as the incident mode in (19). Note that the term multiplied by B_n in (15) has been omitted from (18) so as to eliminate fields that arrive at the observation point after a round trip to the center of the resonator; such fields are not relevant for determination of edge reflection. One observes that $\Gamma_{jn}=0$ for odd values of $j+n$, in conformity with requirements imposed by structural symmetry. The exponential phase terms in (24) arise because the phase reference has been taken at the modal caustics; these terms are absent when the phase is referred to the edges at $\zeta=\bar{\zeta}$. The coupling coefficient Γ_{jn} in (24) represents the lowest order approximation of the ray-optical solution wherein only single (primary) diffraction at the edges is accounted for. This result could be improved by inclusion of multiple diffraction that occurs between the edges, but the effect is small since the ratio of multiple to primary diffraction is $O[(2kL)^{-1/2}]$. The formula in (24) is valid provided that $\beta_n+\beta_j\not\approx\pi$, i.e., the characteristic mode angle β_n does not lie in the reflected-ray transition region associated with the ray incident at the angle β_j. Moreover, for validation of primary diffraction as the dominant mechanism, one edge should not lie in the reflected-ray transition region of the other (this condition is more stringent than the one for $\beta_n+\beta_j$). The necessary restrictions are derived in Appendix II.

B. Simplification for Moderate Fresnel Numbers

To check whether the general coupling coefficient in (24) reduces to the local parallel-plane approximation for small enough Fresnel numbers, and in particular for weakly curved mirrors (small γ in (5c)), the limiting form of (24) in that parameter range is now examined. As noted earlier, the modes of interest are those with caustics near the center of the resonator. Thus the edges may be taken to lie far enough from the caustics to justify $\mu_{cn,j}\ll\bar{\mu}$. Moreover, $\bar{\mu}$ itself is small. When these approximations are introduced, one finds:

$$V(\beta_n,\beta_j)\approx(\operatorname{sgn}\beta_n)(\operatorname{sgn}\beta_j)\cdot\frac{4\bar{\mu}\cos\eta_1}{(2\bar{\mu}^2+1-b_n^2)+(2\bar{\mu}^2+1-b_j^2)}\tag{25a}$$

$$\ln M\approx 2\gamma^{1/2},\qquad\alpha\approx\gamma,\qquad N_{n,j}^2\approx\alpha^{1/2}\tag{25b}$$

$$\bar{\mu}\left(1-\frac{\mu_{cn}^2}{2\bar{\mu}^2}\right)\approx(\bar{\mu}^2-\mu_{cn}^2)^{1/2}=(2/h)^{1/2}\phi_n(\bar{\zeta}).\tag{25c}$$

Thus, when the phase reference is at the edges, (24) reduces to

$$\Gamma_{jn}\approx-i[(s_n+s_j)(s_ns_j)^{1/2}]^{-1},\qquad s_n=2\alpha^{1/4}\phi_n(\bar{\zeta})\tag{26a}$$

and

$$\Gamma_{jj}\approx-\frac{i}{2s_j^2}.\tag{26b}$$

If account is taken of the normalization of the incident field as in (19a), these expressions agree with the parallel-plane formulas of Weinstein [12] for the case where β_n and β_j differ sufficiently from $\pi/2$ to ensure that one edge does not lie in the reflected-ray transition region of the other. In that event, single-edge diffraction is adequate to describe reflection from the open-ended parallel-plane structure. As noted previously [9], s_n represents the modal propagation coefficient in the equivalent parallel-plane waveguide whose height equals that of the hyperbolic waveguide at $\bar{\zeta}$.

When γ is reduced further so that one edge does lie in the reflected-ray transition region of the other edge, interaction between the edges in the local parallel-plane model cannot be ignored. The single-edge diffraction function must now be replaced by a more accurate function derived from the rigorous solution of the semi-infinite parallel-plane configuration. The result as given by Weinstein [20], modified to account for the different normalization of the incident field used here, is as follows:

$$\Gamma_{jn}=-i[(s_n+s_j)(s_ns_j)^{1/2}]^{-1}\exp[U(s_n,\delta)+U(s_j,\delta)]\tag{27}$$

where δ is defined by any of the equalities

$$\frac{2\pi(\hat{j}+\delta)}{\ln M}=p_n=\frac{h}{2}(b_n^2-1)=\frac{n\pi-2kL}{\ln M},\qquad\hat{j}=0,\pm1,\pm2,\cdots.\tag{27a}$$

The diffraction function $U(s,\delta)$ is discussed in detail in [20], and has the following asymptotic behavior:

$$U(s,\delta)\sim 0,\qquad s\text{ large}\tag{28a}$$

$$U(s,\delta)\sim-\frac{1}{2}\left(\ln 2+\frac{i\pi}{2}\right)+\ln(2s)-\frac{1-i}{2}\bar{\beta}s+\cdots,\qquad s\text{ small}\tag{28b}$$

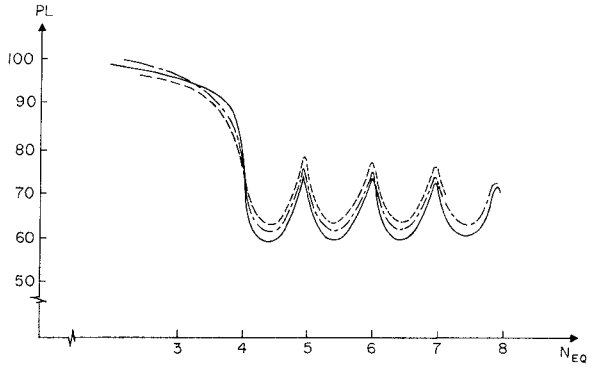

Fig. 3. Ratio W of $|\Gamma_{nn}|$ in (24) to $|\Gamma_{nn}|$ in (26), with $p_n = 0$ (minimum mode loss condition). The calculation is carried out for the parameters $\bar{n} = 100$, $\gamma = 0.4$ as in [10].

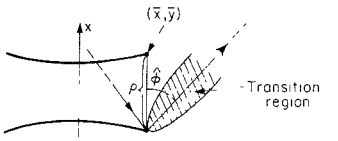

Fig. 4. Power loss PL in the detached eigenmode of a hyperbolic strip resonator. The calculation is carried out for $\bar{n} = 100$, $\gamma = 0.4$ as in [10]. ——— use of (26b). — — — use of (24). - - - - Sanderson and Streifer [25].

where $\bar{\beta} = 0.824$. Thus (27) reduces to (26a) when $s_{n,j}$ are sufficiently large (note that this condition can be met although γ is small). For small $s_{n,j}$, one has

$$\Gamma_{jn} = -2(s_n + s_j)^{-1}(s_n s_j)^{1/2} \exp\left[\frac{-(1-i)\bar{\beta}(s_n + s_j)}{2}\right] \quad (29)$$

which (noting that $s_n \approx s_j$ here) was used in the analysis by Chen and Felsen [9]. With formulas (24) and (27), noting the overlap region in (26a), one may cover the entire range of parameters from small to large Fresnel numbers for the hyperbolic mirror resonator.

To ascertain the effect of the improved reflection coefficient in (24), we have calculated the ratio W of $|\Gamma_{nn}|$ in (24) to that in (26b). One observes from Fig. 3 that W deviates substantially from unity even for moderate values of the equivalent Fresnel number N_{eq} (for a definition of N_{eq}, see (34a)). Corresponding data for the losses in the "detached" eigenmode [25] are plotted in Fig. 4. It is noted that use of the reflection coefficient in (24) yields results which agree more closely with the numerical solution of Sanderson and Streifer [25] than those obtained from (26b). Although the discrepancy in Fig. 3 between $|\Gamma_{nn}|$ in (24) and (26b) is considerable, the effect on the detached resonant mode losses in Fig. 4 is relatively small because Γ_{nn} is $O(10^{-2})$ in that parameter regime. Nevertheless, the results confirm the assertion that use of the ray optically determined reflection coefficient in (24) is expected to yield an improvement over previously available formulations, especially for large Fresnel numbers.

C. Effects of Smoothed Edges or Tapered Reflectivity

The dependence of Γ_{jn} in (24) on $V(\beta_n, \beta_j)$ implies that the nth mode reflected field is proportional to the strength of the edge diffraction pattern along the direction of propagation of the local modal plane-wave constituents in that mode. If the edges can be shaped so that diffraction along β_n is minimal, then the resonant properties of the nth mode in the open-ended waveguide should approach those in a waveguide with infinite mirrors. Since the infinite-mirror configuration has been investigated independently, it is of interest to establish that the resonant fields derived for finite sharp-edged mirrors reduce to those for infinite mirrors as Γ_{jn} tends to zero. This transition is performed in Appendix III.

V. Conclusions

A previously developed ray-optical analysis of scattering by edge discontinuities in a parallel-plane waveguide has here been generalized to curved waveguide boundaries. When both boundaries are convex as in a hyperbolic waveguide, and when the waveguide is truncated bilaterally and symmetrically, the resulting doubly open-ended structure has found application as an unstable optical resonator. For the determination of the resonant properties of this open cavity, it is necessary to know the mode reflection and coupling effects introduced by the edges. This has been done by a generalized ray-optical technique. Accounting only for primary edge diffraction, the resulting modal reflection and coupling coefficients have been shown to be adequate for resonators with large Fresnel numbers, because the contribution from multiple edge diffraction is negligibly small. The expressions so obtained are expected to be more accurate than others employed heretofore (see Fig. 4). As the Fresnel number is decreased, the modal reflection and coupling coefficients reduce to those calculated for an equivalent local parallel-plane geometry near the edges, thereby providing a smooth transition from the case of slanted, to that of parallel boundary contours near the edges. While only open-ended reflection has been treated here, the method applies also to bifurcations, apertures, obstacles, etc. (for these applications, see [7], [21]). The ray-optical approach to edge diffraction introduces a viewpoint not usually associated with obstacle scattering in waveguides. While ray optical considerations have been employed for the unstable resonator [8], [14]–[16] they have not previously been incorporated into a systematic modal theory.

Because the diffraction process is localized near the edges, the results presented here are applicable also to other waveguide boundary shapes, provided that the change in the waveguide cross section occurs sufficiently slowly, in terms of the wavelength scale, to justify use of the WKB approximation for the wave functions. Moreover, subject to similar criteria of slow variability, the method also accommodates resonators filled with variable and/or active dielectrics. These aspects are presently under study, and some results may be found in [27].

APPENDIX I

Determination of Propagation Directions of Modal Local Plane Waves

In the elliptic coordinate system of Fig. 2, the WKB phases $kS_{\eta j}$ and $kS_{\mu j}$ of the wave functions for the jth mode in the η and μ domains are, respectively,

$$kS_{\eta j} = h \int^{\eta} \psi_j(\tau)\, d\tau, \qquad kS_{\mu j} = h \int^{\mu} \bar{\phi}_j(\xi)\, d\xi \tag{30}$$

where $h = kd$, $\bar{\phi}_j(\mu) = (\cosh^2 \mu - b_j^2)^{1/2}$ and $\psi_j(\eta)$ is given in (5). The modal ray congruences for $y > 0$ are directed along $\nabla S_j^{\pm}$, where $S_j^{\pm} = S_{\mu j} \pm S_{\eta j}$. The angle β_j^+ between an incident modal ray and the boundary at $\eta = \eta_1$ is given by

$$\begin{aligned} \cos \beta_j^+ &= \boldsymbol{\mu}_0 \cdot \nabla S_j^+ \\ &= (\cosh^2 \mu - b_j^2)^{1/2} (\cosh^2 \mu - \sin^2 \eta_1)^{-1/2} \end{aligned} \tag{31}$$

where $\boldsymbol{\mu}_0$ is the unit vector along μ. When $\mu = \bar{\mu} \ll 1$, this expression reduces to (20).

APPENDIX II

Restrictions for Applicability of the Diffraction Coefficient in (22)

The exterior of the reflected-ray transition region for the case of a plane wave incident at the angle ϕ_0 on a perfectly conducting half-plane is given by [19] (in this Appendix, ϕ denotes the angular coordinate)

$$\sqrt{\rho}\, |\phi - \phi_0| > \sqrt{\frac{2}{k}} Q \tag{32}$$

where Q is a constant of the order of unity; ρ and $\hat{\phi} = |\phi - \phi_0|$ are polar coordinates with respect to the edge, with $\hat{\phi}$ measured from the reflected-ray direction ϕ_0.

If one edge of the resonator of Fig. 1 is to be outside the reflected-ray transition region of the other edge, then (32) has to be satisfied for ρ and $\hat{\phi}$ as indicated in Fig. 5. Introducing the approximation that the edges of the resonator are located at $\bar{x} = \pm d \sin \eta_1$, which supposes $\bar{\mu} \ll 1$, we find for the case $b_j = 1$, i.e., when the modal caustic degenerates into a straight line between the foci (this is relevant near loss minima of a resonant mode [9], [10]):

$$\rho = 2d \sin \eta_1 \tag{33a}$$

$$\tan \hat{\phi} = \frac{\bar{y}}{d(1 - \sin \eta_1)} \approx \hat{\phi}. \tag{33b}$$

Insertion of (33a) and (33b) into (32) yields the following condition for applicability of the diffraction coefficient in (22):

$$N_{eq} > \frac{Q^2 \alpha^{1/2}}{2\pi\gamma} (1 + 2\gamma - 2\alpha^{1/2}) \tag{34}$$

where N_{eq} is the equivalent Fresnel number

$$N_{eq} = \frac{N}{2}\left(M - \frac{1}{M}\right) \tag{34a}$$

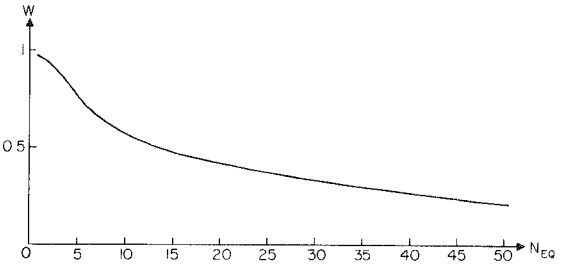

Fig. 5. Reflected ray transition region.

N is the ordinary Fresnel number, and M is defined in (5c). The relations

$$\sin \eta_1 = \left(1 + \frac{1}{\gamma}\right)^{-1/2} \qquad \gamma d = L\alpha^{1/2} \tag{34b}$$

were used in the derivation of (34).

To give some indication of the restriction implied in (34), we note, for example, that for $Q = 3$ and $\gamma = 0.4$, one finds $N_{eq} > 0.813$. Thus (22) applies even for relatively small values of N_{eq}.

APPENDIX III

Resonant Mode Solutions for Mirrors with Smoothed Edges

If the mirror edges at $|\zeta| = \bar{\zeta}$ in Fig. 1 are perturbed, or if a tapered-reflectivity boundary is joined to the waveguide in the region $|\zeta| > \bar{\zeta}$, the analysis presented here remains applicable provided only that $V(\beta_n, \beta_j)$ in (24) is replaced by the diffraction coefficient appropriate to the modified edge discontinuity. Because the intricate patterns of resonant-mode losses and resonant-mode fields are attributable to the strong diffraction caused by sharp-edged mirrors, there has been considerable interest in assessing the effects of a reduction of edge scattering [14]–[16]. In particular, if edge diffraction back toward the foci at $x = \pm d$ in Fig. 1 can be eliminated, the resulting resonant-mode field should be well approximated by the geometric optical field comprised of two cylindrical waves emanating from the foci [22]. The relation between this geometric optical approximation and the modal fields in the hyperbolic waveguide has been established previously [9]. We now show how the resonant mode solutions reduce to those in an infinite waveguide when the edge configuration is shaped so that $V(\beta_n, \beta_j) = 0$.

The resonant field in mode n is given by (edge-coupling to other modes can be neglected when losses in mode n are at a minimum [9], [10]):

$$f_n(\zeta) = f_n^{(1)}(\zeta) + \Gamma_{nn} f_n^{(2)}(\zeta), \qquad \zeta > 0 \tag{35}$$

where $f_n^{(1)}$ and $f_n^{(2)}$ represent waves traveling in the direction of increasing and decreasing ζ, respectively. When $\Gamma_{nn} = 0$, the resonant mode solution becomes $f_n^{(1)}(\zeta)$, which may be identified with $\tilde{F}_n = D_\nu(z)$ (see (10)), provided that p_n is chosen so as to satisfy the modal resonance equation [9], [10]

$$\tilde{R}_n(\zeta_{cn}) \Gamma_{nn} = 1 \tag{36}$$

where the phase reference has been taken at ζ_{cn}. With $\Gamma_{nn} = 0$, it is required that $\tilde{R}_n = \infty$ in (14). Referring to (12),

one observes that this condition implies $\Gamma(\frac{1}{4} + ip_n/2) = \infty$ or

$$p_n = i(\tfrac{1}{2} + 2m), \qquad m = 0, 1, 2, \cdots \tag{37}$$

whence $v \to v_m = -\frac{1}{2} - ip_n = 2m$. In terms of the eigenvalues Ω of the resonator integral equation, one has

$$\Omega = \exp(ip_n \ln M) = M^{-(1/2)-2m} \tag{38}$$

in agreement with the geometric optical calculation [23]. For the lowest mode $m = 0$, one has

$$D_0(z) = \exp(i\zeta^2/4) \tag{39}$$

which is again in accord with the geometric optical field [23]. For the higher order modes $m > 0$, one obtains the known infinite mirror solution involving Hermite polynomials with complex argument [24].[3]

References

[1] H. Y. Yee, L. B. Felsen, and J. B. Keller, "Ray theory of reflection from the open end of a waveguide," *SIAM J. Appl. Math.*, vol. 16, pp. 268–300, 1968.

[2] D. V. Batorsky and L. B. Felsen, "Ray-optical calculation of modes excited by sources and scatterers in a weakly inhomogeneous duct," *Radio Sci.*, vol. 6, pp. 911–923, 1971.

[3] J. J. Bowman, "Comparison of ray theory with exact theory for scattering by open waveguides," *SIAM J. Appl. Math.*, vol. 18, pp. 818–829, 1970.

[4] J. Boersma, "Ray-optical analysis of reflection in an open-ended parallel-plane waveguide: II—TE case," *Proc. IEEE*, vol. 62, pp. 1475–1481, 1974.

[5] S. W. Lee, "Ray theory of diffraction by open-ended waveguides: I. Field in waveguides," *J. Math. Phys.*, vol. 11, pp. 2830–2850, 1970.

[6] L. W. Chen and L. B. Felsen, "Ray method for scattering by discontinuities in a multiwave waveguide," *SIAM J. Appl. Math.*, vol. 27, pp. 138–158, 1974.

[7] D. V. Batorsky and L. B. Felsen, "Scattering by obstacles in an inhomogeneously filled waveguide," *Radio Sci.*, vol. 8, pp. 547–557, 1973.

[3] While the higher order modes in a resonator with reflectionless edges behave as though the mirrors are infinitely large, the validity of these solutions for the infinite mirror geometry has been questioned [25], [26].

[8] A. E. Siegman, "Unstable optical resonators for laser applications," *Proc. IEEE*, vol. 53, pp. 277–286, 1965.

[9] L. W. Chen and L. B. Felsen, "Coupled-mode theory of unstable resonators," *IEEE J. Quantum Electron.*, vol. QE-9, pp. 1102–1113, Sept. 1973.

[10] C. Santana and L. B. Felsen, "Two-dimensional and three-dimensional unstable resonator losses by a waveguide analysis," *Appl. Opt.*, vol. 15, pp. 1470–1478, June 1976.

[11] G. N. Vinokurov, V. V. Lyubimov, and I. B. Orlova, "Investigation of the selective properties of open unstable cavities," *Opt. Spectrosc.* (USSR), vol. 34, pp. 427–432, 1973.

[12] L. A. Weinstein, *Open Resonators and Open Waveguides*. Boulder, Colorado: Golden Press, 1969.

[13] V. V. Lyubimov and I. B Orlova, "Approximate calculation of oscillations in resonators with concave mirrors," *Opt. Spectrosc.* (USSR), vol. 29, pp. 310–313, 1970.

[14] Yu. A. Anan'ev and V. E. Sherstobitov, "Influence of the edge effects on the properties of unstable resonators," *Sov. J. Quantum Electron.*, vol. 1, pp. 263–267, 1971.

[15] V. E. Sherstobitov and G. N. Vinokurov, "Properties of unstable resonators with large equivalent Fresnel numbers," *Sov. J. Quantum Electron.*, vol. 2, pp. 224–229, 1972.

[16] G. L. McAllister, W. H. Steier, and W. B. Lacina, "Improved mode properties of unstable resonators with tapered reflectivity mirrors and shaped apertures," *IEEE J. Quantum Electron.*, vol. QE-10, pp. 346–355, 1974.

[17] L. B. Felsen and N. Marcuvitz, *Radiation and Scattering of Waves*. Englewood Cliffs, NJ: Prentice-Hall, 1973, sec. 3.3.

[18] H. Buchholz, *The Confluent Hypergeometric Function*. New York: Springer-Verlag, 1969.

[19] *Ibid.* [17, sec. 6.5].

[20] L. A. Weinstein, *The Theory of Diffraction and the Factorization Method*. Boulder, CO: Golem Press, 1969, Appendix B and prob. 1.6.

[21] H. Y. Yee and L. B. Felsen, "Ray optics: A novel approach to scattering by discontinuities in waveguide," *IEEE Trans. Microwave Theory Tech.*, vol. MTT-17, pp. 73–85, 1969.

[22] A. E. Siegman, "Unstable optical resonators for laser applications," *Proc. IEEE*, vol. 53, pp. 277–287, 1965.

[23] A. E. Siegman and R. Arrathoon, "Modes in unstable optical resonators and lens waveguides," *IEEE J. Quantum Electron.*, vol. QE-3, pp. 156–163, 1967

[24] L. Bergstein, "Modes of stable and unstable optical resonators," *Appl. Opt.*, vol. 7, pp. 495–503, 1968.

[25] R. L. Sanderson and W Streifer, "Unstable laser resonator modes," *Appl. Opt.*, vol. 8, pp. 2129–2136, 1969.

[26] P. Horwitz, "Asymptotic theory of unstable resonator modes," *J. Opt. Soc. Am.*, vol. 63, pp. 1528–1543, 1973.

[27] C. Santana and L. B Felsen, "Effects of medium and gain inhomogeneities in unstable optical resonators," to be published in *Applied Optics*, vol. 16, pp. 1058–1066, 1977.